Influence of Silica Nanoparticles on the Thermal Transitions and Structure of PHBA/PET Nanocomposites

Félix G. Miranda-Mendoza and Aldo Acevedo[1]

Department of Chemical Engineering, University of Puerto Rico, Mayagüez, PR

ABSTRACT

In this work, we evaluate the effect of spherical silica nanoparticles on the thermal transitions and structure of poly(4-benzoic acid-co-ethylene teraphthalate) (PHBA-PET) films. Composite films were produced by direct melt-blending of the polymer with up to 1.5 vol% loadings in a Thermo-Haake MiniLab2 twin-screw extruder. Thermal transitions were determined by differential scanning calorimetry and thermogravimetric analysis. Structure and morphology were analyzed by a combination of polarized optical microscopy, small-angle x-ray scattering (SAXS), and scanning electron microscopy. No significant changes were observed on the glass transition temperature, nevertheless the melting point showed a small tendency toward higher values at higher loadings. The nematic range decreased upon addition of particles, but was mostly unaffected by concentration. The maximum rate of degradation was displaced up to 30 ºC. A detrimental effect on the internal ordering of the polymer was also observed, as suggested by the reduction of the characteristic SAXS peak. Micrographs show a smooth film surface and straight fracture planes (i.e. no fibrils). Silica particles improved the thermal properties of the polymer, yet as the loading increase results suggest a reduction of the nematic range and order.

Keywords: polymer nanocomposites, liquid crystals, extrusion, silica.

1 INTRODUCTION

Polymer composites have been studied in the last few decades for a wide variety of engineering applications [1-3]. Recently the interest has been focused on systems where filler size lie in the nanometer scale, or nanocomposites [4]. Great improvements on the mechanical and thermal properties, when compared to the neat matrix, have been demonstrated with just minute ammounts of nanoparticles [5, 6]. The improvements in the physical and chemical properties are primarily due to the large surface area per unit volume of the fillers, which allow for enhanced interactions with the matrix molecules.

Liquid crystalline polymers are composed of linear semi-rigid molecules which are capable of forming oriented or anisotropic structures. Specifically polymers that show nematic structures are very attractive for polymer processing techniques such as extrusion, since they have low melt viscosity and can be easily oriented in the flow direction [7]. The interest in studying these systems reside in the potential for producing ligthweight components, while promoting excellent mechanical and thermal performance at lower production costs [8].

In this type of composites, the formation of fibrillar structures is related to composite property enhancement. While structures such as those reported by Quin [9], where ellipsoids and short fibrils were found on Rodrun LC 3000/PP composites, does not promote relevant property improvements. In this work the effect of spherical silica nanoparticles inclusion, at loadings up to 1.5 v%, on the thermal transitions and structure of model thermotropic poly(4-benzoic acid-co-ethylene terephthalate) (PHBA/PET) uniaxial film nanocomposites produced by direct melt blending on a twin screw extruder was studied.

2 EXPERIMENTAL

2.1 Materials

The studied nanocomposites were prepared using the thermotropic liquid crystalline polymer matrix poly (4-benzoic acid-co-ethylene terephthalate) 60:40 mol % (PHBA/PET), and amorphous silica fillers with an average diameter of 15 nm. This polymer is industrially known as Rodrun LC 3000 [9, 10]. Both were purchased from Sigma Aldrich.

2.2 Processing

Nanocomposite films were produced by direct melt blending in a co-rotating intermeshing twin screw extruder (Haake MiniLab II). Polymer pellets and fillers were slowly fed to the extruder for approximately 10 minutes at 290 °C, while screws rotate at 10 rpm in order to perform a pre-mixing and most importantly, to avoid material accumulation at the hopper. The melt was then processed at 40 rpm and 300 °C for approximately 40 minutes. Afterwards, the sample is extruded at 190 °C (close to T_m) and 10 rpm to increase composite viscosity for a better control of film size when exiting the die. The extrudate is collected over a D22 conveyor belt which was manually controlled to match the exiting flow rate.

[1] corresponding author: PO Box 9000, Mayaguez, PR 00680 or aldo.acevedo@upr.edu

2.3 Digital Scanning Calorymetry

Differential scanning calorimetry (DSC) was performed in a TA Instruments Q-2000 DSC to identify the glass (T_g), melting (T_m) and isotropic-to-nematic (T_{IN}) transition temperatures. Random film samples of approximately 10 to 15 mg were deposited in a T_{zero} aluminum pans with hermetic lid. Thermograms were collected in standard mode from 20 to 420 °C at a heating rate of 5 °C/min in a dry atmosphere.

2.4 Thermo Gravimetric Analysis

Non-isothermal analyses were carried out using a TA Instruments Q-2950 thermo gravimetric analyzer (TGA) to determine decomposition temperature of the composites. Samples ranging from 20 to 30 mg were loaded on an aluminum pan and heated at a rate of 5 °C/min from 20 to 600 °C. Air flows of 60 and 40 mL/min were used for the sample and reference chamber, respectively.

2.5 Polarized Optical Microscopy

Polarized optical microscopy was used to coonfirm the nematic phase range determined by DSC. Samples were analyzed in a Olympus BX-51 equiped with an Instec thermal hot stage. Micrographs were taken at a magnification of 40× and recorded with a Cannon professional digital camera. The observed samples were cut with a surgical blade from surface to inner sections to have a representative look at the bulk.

2.6 Scanning Electron Microscopy

Scanning electron micrographs were obtained using a JEOL-JSM-6930LV at an accelerating voltage of 10 kV. Composite samples were randomly broken to study their fracture planes. Samples were coated with gold in a spun coater for approximately two minutes as recommended for the low conductive samples. Sample pieces were placed over carbon glue grids and aluminum pan holders. The surface of the composites was also scanned.

2.7 Small Angle X-ray Scattering

The effect of the silica nanoparticles on the matrix morphology was studided in the small angle X-ray range using a SAXS attachment for a Rigaku Ultima III theta-theta goniometer unit with a CuK_{α} target (λ= 1.5418 Å). The anode was operated at 40 kV and 44 mA. Also a divergence slit and a high limitting slit of 1.0 mm and 10.0 mm, respectively, were used along with a sample holder attachment for transmission method. A scanning speed of 0.05 °/min at steps of 0.05 ° were used to obtain patterns in the 2 theta range from 0.6 to 1.5 °.

3 RESULTS AND DISCUSSION

3.1 Thermal Characterization

DSC thermograms for the neat PHBA/PET matrix and composites, shown in Figure 1, show three thermal transitions. The first transition appears around 50 °C and was identified as the glass transition (T_g). The second transition is around 180 °C and corresponds to the melting of crystallites (T_m). Finally above the 300 °C, the temperature reaches a maximum peak, identified as the characteristic temperature for the isotropic-to-nematic phase transition (T_{IN}). The transition temperatures for the polymer matrix and nanocomposites are summarized in Table 1. The characteristic temperatures for these transitions were obtained using the Universal Analysis software by taking the minimum peak temperature for the endothermic glass and melting transitions, and the maximum peak temperature of the exothermic isotropic-to-nematic transition.

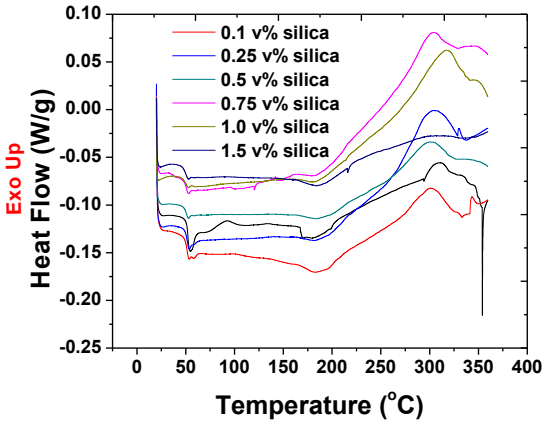

Figure 1: DSC thermograms of PHBA/PET silica nanocomposites.

silica (v%)	T_g (°C)	T_m (°C)	T_{IN} (°C)
neat	52.5	184.2	330.0
0.10	53.0	182.4	302.3
0.25	53.5	186.8	301.8
0.50	52.5	198.2	300.9
0.75	52.4	192.4	304.1
1.00	54.8	193.0	307.0
1.50	51.3	185.2	302.0

Table 1: Transtition temperatures for PHBA/PET silica nanocomposites.

Addition of silica nanoparticles does not have a significant effect on the glass transition temperature since it remains almost constant. While the melting point shows an increment from medium to high concentrations (0.5 – 1.0 v%), which may be attributed to the interactions between the polymer chains and the nanoparticles, which causes a reduction of the macromolecular chain mobility around the nanoparticles. On the other hand, the temperature range where the liquid crystalline phase lies is supresed since the peak temperature (at nematic phase) decreases from 330 °C for the neat matrix to values ranging from 300 to 307 °C, independent of loading.

Comparing the transition enthalpies, summarized in Table 2 and determined as the area under the curve obtained using the Universal Analysis software, it can be deduced that addition of silica nanoparticles lowers the enthalpy of the glass transition. This may be attributed to the imperfections caused by the particles on the semicrystalline lattice of the matrix. The latter translate into a lower energy requirement in order to pass from a solid state to a more relaxed system, since some disorder has been introduced to the system by the spherical fillers. This effect is more evident as particle concentration was increased, but at lower particle loadings (i.e. 0.1 & 0.25 v%) thermal stability was promoted.

silica (v%)	ΔH_g (J/g)	ΔH_m (J/g)	ΔH_{IN} (J/g)
neat	1.01	3.54	1.25
0.10	1.17	2.40	11.12
0.25	1.29	1.78	19.12
0.50	0.45	4.35	12.22
0.75	0.59	3.59	12.89
1.00	0.31	2.89	12.74
1.50	0.50	1.94	12.48

Table 2: Transition enthalpies for PHBA/PET silica nanocomposites.

The heat of fusion (i.e. enthalpy at the melting point) does not show a trend with the addition of silica, since a random behavior was observed. For the enthalpy associated with nematic phase transition a significant change, at least a factor of 10, was observed as silica is added. A higher attraction between the silica surface and the polymer may distort the liquid crystalline ordering, but remaining nematic regions are confined between particles.

PHBA/PET degrades in two stages corresponding to each of its monomeric units, as shown in Figure 2. The first stage corresponds to the degradation of ET units, while the second stage is due to decomposition of HBA. From the thermogravimetric analysis curves it can be deduced that the addition of silica nanoparticles improve composite thermal stability, since there is a displacement on the degradation stages toward higher temperatures with increasing particle loading. Figure 3 summarizes the degradation temperatures for both stages, taken at the point of maximum degradation rate. A displacement toward higher values is observed in both cases. This may be attributed to the formation of hydrogen bonds beteween the SiO_2 and the carboxyl groups of the PHBA and PET units. This interfacial affinity between particle and matrix molecules may improve the thermal properties of the composites.

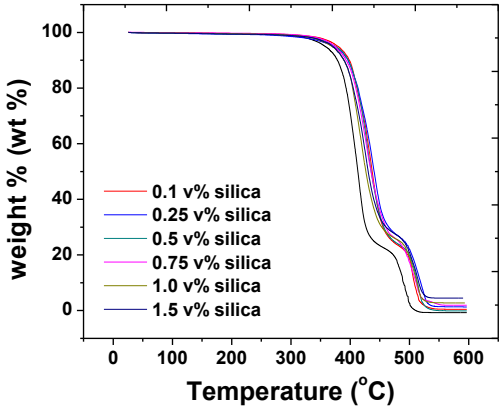

Figure 2: Thermogravimetric characterization of PHBA/PET silica nanocomposites.

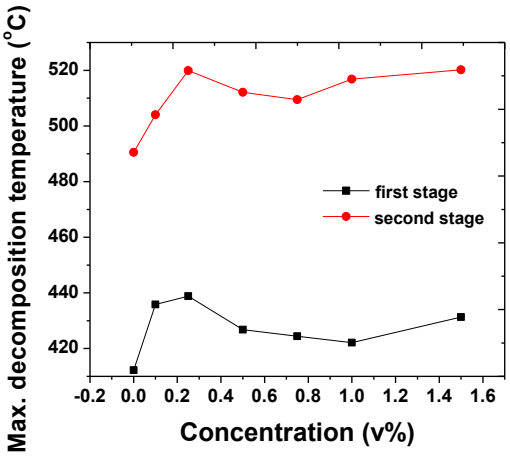

Figure 3: Effect of silica nanoparticles on characteristic decomposition temperatures.

3.2 Structure and Morphology

POM confirmed nematic ordering of the composites within the range determined by DSC. Figure 4 shows sample micrographs of the neat polymer and some silica nanocomposites at 300 °C. The reported photos were taken close to the maximum temperature of the nematic-to-isotropic phase transition. There was neither significant changes as particle concentration increased nor evidence of particle percolation. Yet, the formation of multiple spherulites is evident, which may be attributed to the silica acting as a nucleating agent. In this melt state, the

deformation of molecules near particle surface is known to show this behavior [11].

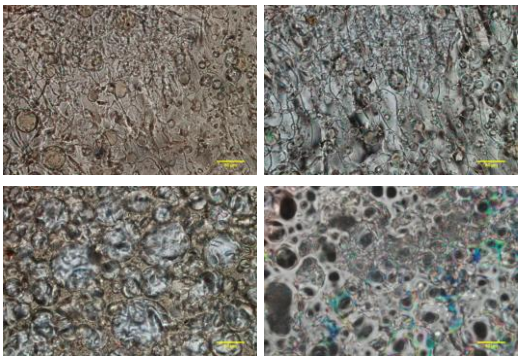

Figure 4: POM photos of LC phase of neat polymer (top left), and silica composites of 0.25 (top right), 0.50 (bottom left), and 1.50 (bottom right) v% at 300 °C and magnification of 40X.

Another analysis performed on the composite was the study of surface and fracture planes by SEM, as the example shown in Figure 5. No fibrilar surfaces were identified. Instead, the formation of circular structures (voids) and smooth film surface were observed. This type of structure suggests poor mechanical properties, since the particles do not provide resistance to failure or crack propagation.

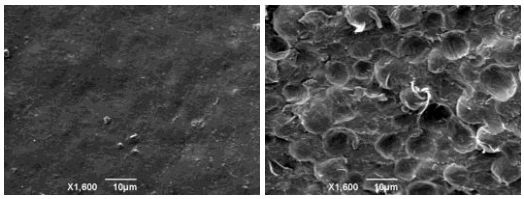

Figure 5: Film surface (left) and fracture plane (right) of PHBA/PET with 0.25 v% silica.

SAXS difractograms are shown in Figure 6. No difference in peak position was observed within the studied particle loading range. Thus, no change in the LC ordering was promoted by the addition of the silica nanoparticles. Yet, a flattenning of the area under the peak might suggest a decrease of the nematic regions. Nevertheless, the changes are small, thus further analysis has to be performed to determine the experimental error of the measurements.

4 CONCLUSIONS

Good filler-matrix compatibility was observed as evidenced by the effect of the silica particles on the transition temperatures (i.e. glass, melting and degradation) and their associated enthalpies. A good dispersion was also supported by the increased number of spherulites in the melt, and the distribution of voids on the fracture planes of the films. The latter suggest a reduction of mechanical properties, due to a loss of nematic ordering which promotes the formation of fibrilar structures. The nematic temperature range was reduced, while SAXS suggest a reduction of the ordering. Yet, the SAXS results are inconclusive. Thus, silica particles can improve the thermal properties of PHBA/PET films, but at the expense of a decrease of nematic ordering which will cause a detrimental effect on the mechanical properties.

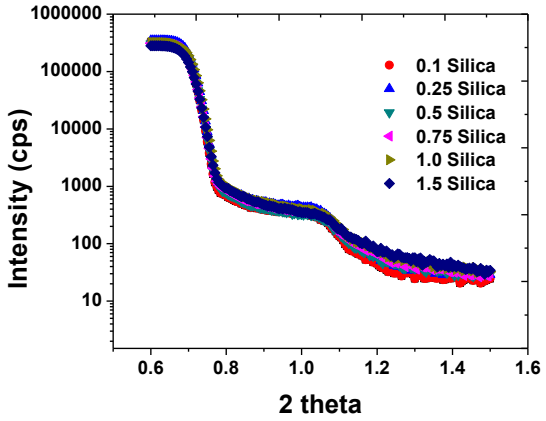

Figure 6: Effect of silica nanoparticles on the SAXS patterns of PHBA/PET nancomposites.

Acknowledgements: This work was partially funded by DMR-0934115 grant of the National Science Foundation.

REFERENCES

[1] R. A. Vaia and E. P. Giannelis, *Polymer*, vol. 42, pp. 1281-1285, 2001.

[2] S. Pavlidou and C. D. Papaspyrides, *Progress in Polymer Science*, vol. 33, pp. 1119–1198, 2008.

[3] H. M. C. d. Azeredo, *Food Research International*, vol. 42, pp. 1240–1253, 2009.

[4] S. S. Ray and M. Okamoto, *Progress in Polymer Science*, vol. 28, pp. 1539–1641, 2003.

[5] L. Bistric˘ic´, G. Baranovic´, M. Leskovac, and E. G. i. Bajsic´, *European Polymer Journal*, vol. 46, pp. 1975–1987, 2010.

[6] Y.-L. Liu, C.-Y. Hsu, W.-L. Wei, and R.-J. Jeng, *Polymer*, vol. 44, pp. 5159–5167, 2003.

[7] M. W. Lee, X. Hu, L. Li, C. Y. Yue, K. C. Tam, and L. Y. Cheong, *Composites Science and Technology*, vol. 63, pp. 1921–1929, 2003.

[8] R. Pfaendner, *Polymer Degradation and Stability*, vol. 95, p. 369e373, 2010.

[9] Y. Qin, D. Brydon, R. Mather, and R. Wardman, *Polymer*, vol. 34, pp. 3597–604, 1993.

[10] L. Incarnato, O. Motta, and D. Acierno, *Polymer*, vol. 97, pp. 5085-5091, 1998.

[11] M. W. Lee, X. Hu, C. Y. Yue, L. Li, and K. C. Tam, *Composites Science and Technology*, vol. 63, pp. 339-346, 2003.